ISSN XXXX XXXX © 2017 IJESC

Research Article Volume 7 Issue No.5

Texture and Gabor Wavelet Based Classification of Hysteroscopy Images of the Endometrium

Safaa Muthana Sulaiman[1], N. Anupama[2]
M.Tech Student[1], Assistant Professor[2]
Department of Computer Science Engineering
A.N.U. College of Engineering & Technology, Guntur, Andhra Pradesh, India

Abstract:
The objective of this study was to classify hysteroscopy images of the endometrium based on texture analysis and Gaborwavelet for the early detection of gynecological cancer. A total of 418 Regions of Interest (ROIs) were extracted (209 normal and 209 abnormal) from 40 subjects. Images were gamma corrected and were converted to gray scale. The following texture features were extracted: (i) Statistical Features (sf), (ii) Spatial Gray Level Dependence Matrices (SGLDM), and (iii) Gray level difference statistics (GLDS). The PNN and SVM neural network classifiers were also investigated for classifying normal and abnormal ROIs. Results show that there is significant difference (using Wilcoxon Rank Sum Test at a=0.05) between the texture features of normal and abnormal ROIs for both the gamma corrected and uncorrected images. Abnormal ROIs had lower gray scale median and homogeneity values, and higher entropy and contrast values when compared to the normal ROIs. The highest percentage of correct classifications score was 77% and was achieved for the SVM models trained with the SF, GLDS and Gaborwavelet features. Concluding, texture features and Gaborwavelet provide useful information differentiating between normal and abnormal ROIs of the endometrium.

I. INTRODUCTION:

Hysteroscopy is the inspection of the uterine cavity by endoscopy with access through the cervix. It allows for the diagnosis of intrauterine pathology and serves as a method for surgical intervention (operative hysteroscopy) as shown in .fig1.

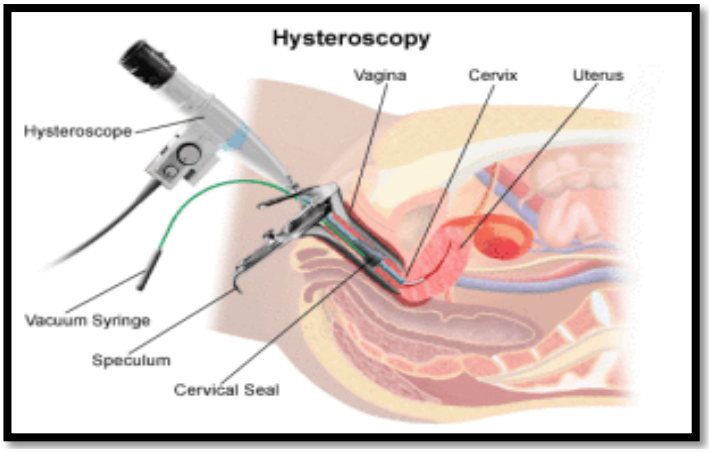

Figure.1. shown image operative hysteroscopy.

A hysteroscopy is an endoscope that carries optical and light channels or fibers. It is introduced in a sheath that provides an inflow and outflow channel for insufflation of the uterine cavity. In addition, an operative channel may be present to introduce scissors, graspers or biopsy instruments.[1] A hysteroscopic resectoscope is similar to a transurethral resectoscope and allows entry of an electric loop to shave off tissue, for instance to eliminate a fibroid.[1][2] A contact hysteroscopy is a hysteroscopy that does not use distention media as shown in fig.2.

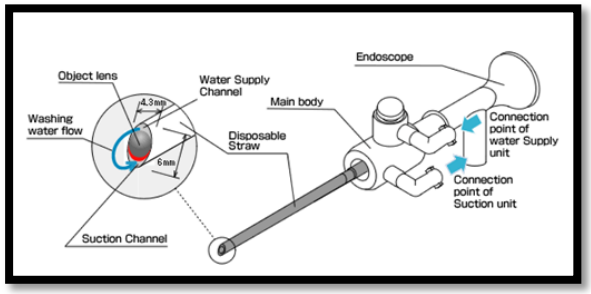

Figure.2. shown image hysteroscopy instruments.

Cancer diseases are the second cause of death in USA with over 557.271 deaths in 2002. Gynecological cancer is the second cause of death among the female population and in 2005 over 40.880 new cases is expected to be diagnosed with an estimation of 7.310 deaths from gynecological caner [1]. In this study, hysteroscopy imaging is investigated for the assessment of endometrium tissue. Hysteroscopy is considered to be the golden standard technique for the diagnosis of intrauterine pathology [2]. The physician guides the telescope connected to a camera inside the uterus in order to investigate suspicious lesions of cancer [3].

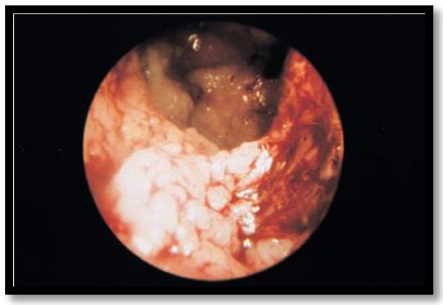

Figure.3. Showing endometrial cancer has spread to the endoservix this image taken by the hysteroscopy.

The objective of this study was to evaluate the usefulness of texture analysis for differentiating between normal and abnormal ROIs from hysteroscopy images of the endometrium for the early detection of gynecological cancer. To the best of our knowledge, no similar study was carried out for hysteroscopy imaging of the endometrium. In previous work, we used the abdominal cavity of a chicken and calf uterus as experimental tissue, comparing texture feature variability under different viewing conditions such as different angles (with 5 degrees difference) and different distances (of 3 cm in close up view and 5 cm in panoramic view) from the ROI under investigation [4]. The results indicated that for small consecutive angles there is no significant difference in texture features analysis but there is significant difference when comparing panoramic vs. close up views. In another study, we demonstrated that some texture features can be used to differentiate between normal and abnormal endometrium images captured during hysteroscopy [5]. However, in both [4] and [5], the images were not gamma corrected. Instead, image intensity normalization was carried out by white balancing, adjusting the camera gain. This approach introduces same sources of variability in the acquisition. Also, in previous work [6] we proposed a standardized protocol for capturing hysteroscopy images using gamma correction as a preprocessing step. The significance of color calibration of the CCD camera was also proposed by [7] and [8]. Scarcanski et al. [8] proposed a hardware calibration protocol of hysteroscopy images with very good results according to the experts. Moreover, the use of color information for the content based retrieval of endoscopy images was also applied successfully by Shunren et al. [9].

- **Hysteroscopy** is a procedure done by a gynecologist or infertility specialist physician that investigates uterine causes of infertility and miscarriages
- It is done by passing a narrow scope through the vagina and cervical opening to visualize the inside of the uterine cavity
- There are various abnormalities that can be found that can interfere with initial embryo implantation, or with ongoing pregnancy.
- These structural abnormalities of the uterine cavity can prevent pregnancy from beginning or they can prevent continuation of pregnancy (increasing the risk for miscarriage).

III. PROPOSED METHODOLOGY:

Block Diagram:

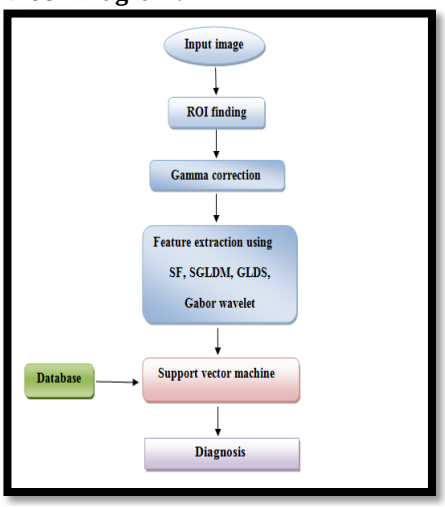

A. Recording of video

The CIRCON IP4.1 [10] medical camera was used. The analog output signal of the camera (PAL 475 horizontal lines) was digitized at 720x576 pixels using 24 bits color at 25 frames per second, and was then saved in AVI format. The Digital Video Creator 120 frame grabber was used.

B. Material

A total of 418 hysteroscopy images from the endometrium were recorded from 40 subjects (see Fig. 1). Regions of Interest of 64x64 pixels were cropped and classified into two categories: (i) normal (N=209) ROIs and (ii) abnormal (N=209) ROIs based on the physician opinion and the histopathological examination[11] (see Fig. 2).

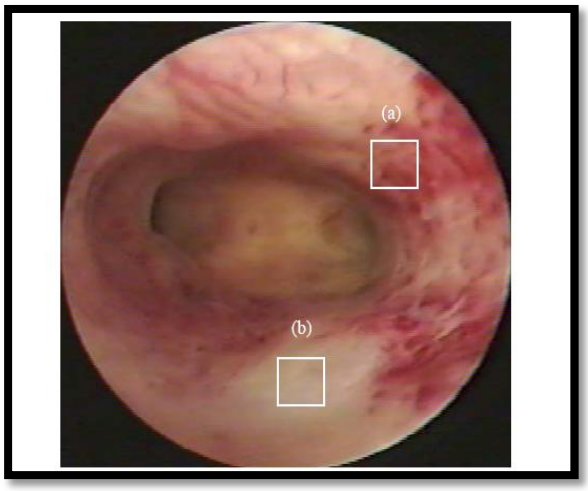

Figure. 4. A hysteroscopy image of the endometrium before gamma correctionwith ROIs selected by the gynecologist: (a) normal ROI, and (b) abnormal ROI.nodules

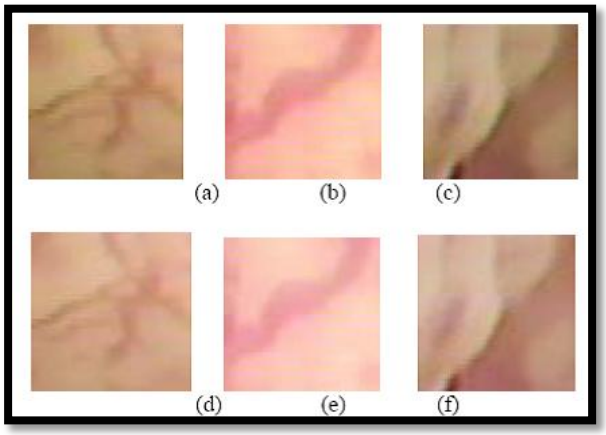

Figure.5. ROIs of the endometrium. Original images: (a) normal tissue (b) and (c) abnormal tissue. Corresponding gamma corrected images (d) normal tissue (e) and (f) abnormal tissue

C. Gamma correction

Most of the cameras have a nonlinear relationship between the signal voltage and the light intensity. The light intensity input to the medical camera or the output of the display is proportional to the voltage raised to the power gamma. Gamma is computed

using calibration color images, and then applying a non linear fitting. Gamma is computed for the red, green and blue channels, and typical values used by our group based on previous findings were in the range of 1.4 to 1.6 [6].

D. Feature Extraction

ROIs were transformed into grayscale using the equation (Intensity=0.299*red+0.587*green+0.114*blue channels) and the following texture features [12] were computed:

Statistical Features (SF):

SF features describe the gray level histogram distribution without considering spatial independence [18]. The following texture features were computed: 1) Mean, 2) Variance and 3) Entropy,

Spatial Gray Level Dependence Matrices (SGLDM):

The spatial gray level dependence matrices as proposed by Haralick et al. [13] are based on the estimation of the second-order joint conditional probability density functions that two pixels (*k*, *l*) and (*m*, *n*) with distance *d* in direction specified by the angle θ, have intensities of gray level *i*and gray level *j*. Based on the estimated probability density functions, the following four texture measures out of the 13 proposed by Haralick et al. [13] were computed: 1) Contrast, 2) Correlation, 3) Homogeneity, 4) Entropy. For a chosen distance *d* (in this work *d=1* was used), and for angles $\theta = 0^o$, 45^o, $90^o$and 135^owe computed four values for each of the above texture measures. The above features were calculated for displacements δ=(0,1), (1,1), (1,0), (1,-1), where δ = (Δx,Δy), and their range of values were computed.

Gray level difference statistics (GLDS):

The GLDS algorithm [14], [15] is based on the assumption that useful texture information can be extracted using first order statistics of an image. The algorithm is based on the estimation of the probability density $p\delta$of image pixel pairs at a given distance δ = (Δx,Δy),, having a certain absolute gray level difference value. Let $p\delta$be the probability density of $f\delta(x,y)$. If there are *m* gray levels, this has the form of an *m*dimensional vector whose *i* the component is the probability that $f\delta(x,y)$ will have value *i*. If the picture *f* is discrete, it is easy to compute $p\delta$by counting the number of times each value of $f\delta(x,y)$ occurs, where (Δx and (Δy are integers. Coarse texture images, result in low gray level difference values, whereas, fine texture images result interpixel gray level differences with great variances. Variable i is two pixels gray level difference, m is the number of gray levels and p$\delta$are the individual probabilities. Features were estimated for the following distances δ =(d,0), (d,d), (-d,d), (0,d). A good way to analyze texture coarseness is to compute, for various magnitudes of δ, some measure of the spread of values in $p\delta$away from the origin.

Gabor Wavelet:

The motivation for Gabor wavelets comes from finding some function $f(x)$ which minimizes its standard deviation in the time and frequency domains. More formally, the variance in the position domain is:

$$(\Delta x)^2 = \frac{\int_{-\infty}^{\infty}(x-\mu)^2 f(x) f^*(x) dx}{\int_{-\infty}^{\infty} f(x) f*(x) dx}$$

where f*(x)is the complex conjugate of $f(x)$ and μ is the arithmetic mean, defined as:

$$(\Delta x)^2 = \frac{\int_{-\infty}^{\infty}(x-\mu)^2 f(x) f^*(x) dx}{\int_{-\infty}^{\infty} f(x) f*(x) dx}$$

The variance in the wave number domain is:

$$(\Delta x)^2 = \frac{\int_{-\infty}^{\infty}(x-\mu)^2 f(x) f^*(x) dx}{\int_{-\infty}^{\infty} f(x) f*(x) dx}$$

Where $k0$ is the arithmetic mean of the Fourier Transform of

$$k0 = \frac{\int_{-\infty}^{\infty} KF(x) F*(x) dk}{\int_{-\infty}^{\infty} KF(x) F*(x) dk}$$

With these defined, the uncertainty is written as:
$(\Delta x)(\Delta k)$

This quantity has been shown to have a lower bound of 1/2. The quantum mechanics view is to interpret(Δx) as the uncertainty in position and as uncertainty in momentum. A function h*(Δk) that has the lowest theoretically possible uncertainty bound is the Gabor Wavelet.[16]

E. Image Classification

The diagnostic performance of the texture features was evaluated classifier Support Vector Machine (SVM). These classifiers were trained to classify the texture features into two classes: i) normal ROIs or ii) abnormal ROIs. This classifier was investigated for several spread radius in order to identify the best for the current problem. The SVM network was investigated using Gaussian Radial Basis Function (RBF) kernels; this was decided as the rest of the kernel functions could not achieve so good results. The SVM with RBF kernel was investigated using 10-fold cross validation in order to identify the best parameters such as spread of the RBF kernels [17]. The leave-one-out method was used for validating all the classification models. A total of 418 runs were carried out for training the classifiers, and the performance of the classifiers was evaluated on the remaining one subset. The performance of the classifier systems were measured using the parameters of the receiver operating characteristic (ROC) curves [17]: true positives (TP), false positives (FP), false negatives (FN), true negatives (TN), sensitivity (SE), specificity (SP), and precision (PR). We also computed the percentage of correct classifications ratio (%CC) based on the correctly and incorrectly classified cases. The time performance of the PNN was 60 sec and the time performance for the SVM algorithm was 10 min.

III. RESULTS:

Results are obtained as shown in fig below by using both svm and pnn

Firstly create gui as shown in figure below.

Figure.1. GUI of The Main Program images

Nowwe press on the 'feature training' bottom then we go to 'read test image' selection to choose the image We want to test it then we press 'ROI selection' bottom to crop the region that we think its infected. Now extract the feature extraction by pressing, now select different feature extraction technique and press svm classification for identifying the disease. As shown in fig 4

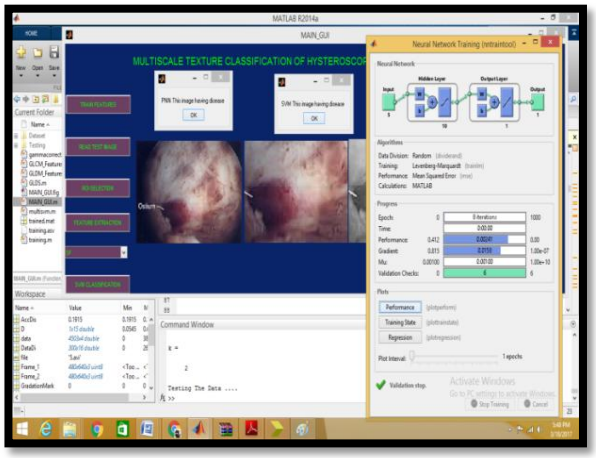

Figure.2. Performing PNN and SVM Classification

Now it is finally showing PNN based and SVM based classifying results and showing results regarding disease.

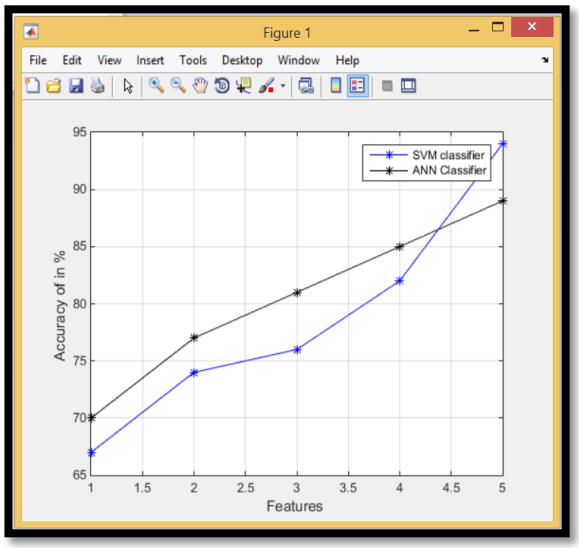

Figure.3. this figure showing the accuracy in % with ANN and SVM classifier

Table.1.the accuracy for the features above with SVM and ANN classifier

	SVM classifier	ANN classifier
SGLDM	68.00000	71.00000
GLDS	73.00000	74.00000
SF+SGLDM+GLDS	76.00000	79.00000
SF+GLDS	82.00000	79.00000
SF+GLDS+GBW	91.00000	87.00000

In (table 1) we can see that by using **Gabor wavelet** feature the accuracy increased more than by using **SGLDM** feature in both SVM and ANN classifier

IV. CONCLUSION:

In this study we classified ROIs of the endometrium from hysteroscopy images based on texture features before and after gamma correction. Results showed that the gamma corrected color images were visually better than the originals according to the gynecologist opinion. There was a significant difference in the SF, SGLDM, and GLDS features investigated between the normal and abnormal ROIs. The highest percentage of correct classifications score was 77% and was achieved for the SVM classifier for the SF+GLDS feature sets. These results support the application of texture analysis for the assessment of difficult cases of normal and abnormal ROIs for gynecological cancer. thegynecologist during the operation so as to identify suspicious ROIs for further histopathological examination. Future work will also investigate multiscale color texture analysis in differentiating between normal and abnormal ROIs of the endometrium.

V. REFERENCES:

[1]. Lin BL, Iwata Y, Liu KH, Valle RF. The Fujinon diagnostic fiber optic hysteroscopy. *J Repro Med*. 1990; 35:685-9.

[2]. J.A. Fayez, M.F. Vogel, "Comparision of different treatment methods of end ometriom as by laparoscopy," Obstet. Gynecol., Vol. 78, pp.660-665, 1991.

[3]. R. Wenzl, R. Lehner, U. Vry, N. Pateisky, P. Sevelda, P. Husslein, "Three-dimensional video-hysteroscopy: clinical use ingynaecological laparoscopy," Lancet, Vol. 344, pp. 1621–1622, 1994.

[4]. M.S. Neophytou, C.S. Pattichis, M.S. Pattichis, V. Tanos, E. Kyriacou,D. Koutsouris, "Multiscale Texture Feature Variability Analysis in Hysteroscopy Imaging Under Different Viewing Positions," Proc. IIEFOMP Med. Conf. on Med. Phys., Limassol, Cyprus, 2004.

[5]. M.S. Neophytou, C.S. Pattichis, M.S. Pattichis, V. Tanos, E. Kyriacou,S. Pavlopoulos, D. Koutsouris, "Texture Analysis of the EndometriumDuring Hysteroscopy: Preliminary Results," Proc. IEEE EMBS 04Conf., San Francisco, USA, Sep. 2004.

[6]. M.S. Neophytou, C.S. Pattichis, M.S. Pattichis, V. Tanos, E. Kyriacou,D. Koutsouris, "The Effect of Color Correction of Hysteroscopy Images for Quantitative Analysis in

Endometrium,"27th Annual International conference of the IEEE engineering in Medicine and Biology Society, 1-4 September, Shanghai, China, 4 pages, 2005.

[7]. S. Sheraizin, V. Sheraizin, "Endoscopy Imaging Intelligent Contrast Improvement" 27th Annual International conference of the IEEE engineering in Medicine and Biology Society, 1-4 September, Shanghai, China, 4 pages, 2005.

[8]. J. Scarcanski, W. Gaviao, S. Cunha, F. Joao, "Diagnostic Hysteroscopy Video Summarization and Browsing", 27th AnnualInternational conference of the IEEE engineering in Medicine andBiology Society, 1-4 September, Shanghai, China, 4 pages, 2005

[9]. X. Shunren, M. Weirong, W. Xiaoying, Z. Zanchao, "A content-Based retrieval system for Endoscopic Images", 27th Annual International conference of the IEEE engineering in Medicine and Biology Society,1-4 September, Shanghai, China, 4 pages, 2005.

[10]. Ong L, De Haes J, Hoos A, Lammes F. Doctor-patient communication: a review of the literature. Social Science &Medicine. 1995;40(7):903–18.

[11]. Creasman WT (1997) Endometrial cancer: incidence, prognostic factors, diagnosis, and treatment. SeminOncol 24: S1-140-S1-50.

[12]. P.M. Tjoa, M.S. Krishnan, "Feature extraction for the analysis of colon status from the endoscopic images," Bio Medical Engineering On Line, Apr. 2003. Available: http://www.biomedical-engineeringonline.com/content/2/1/9.

[13]. R.M. Haralick, K. Shanmugam, I. Dinstein, "Texture Features for Image Classification," IEEE Trans. on Systems, Man., and Cybernetics, Vol. SMC-3, pp. 610-621, Nov. 1973.

[14]. C.M. Wu, Y.C. Chen, and K.S. Hsieh, "Texture features for classification of ultrasonic liver images," IEEE Trans. Med. Imaging,vol. 11, pp.141-152, 1992.

[15]. J.S. Wenska, C.R. Dryer, and A. Rosenfeld, "A comparative study of texture measures for terrain classification," IEEE Trans. Syst., Man, Cyber., vol. SMC-6, pp. 269-285, 1976.

[16]. D.F Specht, Probabilistic Neural Networks, INNS Neural Networks3(1), 109-118, 1990.

[17]. T. Joachims, "Making large-scale svm learning practical. advances inkernel methods - support vector learning". In B. Schölkopf, C. Burges, and A. Smola, editors, Advances in Kernel Methods: Support Vector Machines, pages 169-184. MIT Press, Cambridge, MA, USA, 1999.

[18]. Chandra Mohan M, V. Vijaya Kumar, and U S N Raju, "New Face Recognition Method Based on Texture Features using Linear Wavelet Transforms", IJCSNS International Journal of Computer Science and Network Security, VOL.9 No.12, December 2009.

VI. BIOGRAPHY